Low Temperature Physics

Raman scattering study of the rare-earth binary ferroborate $Nd_{0.75}Dy_{0.25}Fe_3(BO_3)_4$ single crystal

Cite as: Low Temp. Phys. **47**, 1011 (2021); https://doi.org/10.1063/10.0007074
Submitted: 20 October 2021 • Published Online: 21 December 2021

A. Yu. Glamazda, V. P. Gnezdilov, P. Lemmens, et al.

Low Temperature Physics ARTICLE scitation.org/journal/ltp

Raman scattering study of the rare-earth binary ferroborate $Nd_{0.75}Dy_{0.25}Fe_3(BO_3)_4$ single crystal

Cite as: Fiz. Nizk. Temp. **47**, 1107–1118 (December 2021); doi: 10.1063/10.0007074
Submitted: 20 October 2021

A. Yu. Glamazda,[1,2,a)] V. P. Gnezdilov,[1,3] P. Lemmens,[3,4] G. A. Zvyagina,[1] and I. A. Gudim[5]

AFFILIATIONS

[1]B. Verkin Institute for Low Temperature Physics and Engineering of the National Academy of Sciences of Ukraine, Kharkiv 61103, Ukraine
[2]V. N. Karazin Kharkiv National University, Kharkiv 61022, Ukraine
[3]Institute for Condensed Matter Physics, TU-Braunschweig, Braunschweig 38106, Germany
[4]Laboratory for Emerging Nanometrology and International Graduate School of Metrology, TU-Braunschweig, Braunschweig 38106, Germany
[5]L. V. Kirenskii Institute of Physics, Siberian Branch of the Russian Academy of Sciences, Krasnoyarsk 660036, Russia

[a)]**Author to whom correspondence should be addressed:** glamazda@ilt.kharkov.ua

ABSTRACT

We report comprehensive Raman scattering measurements on a single crystal of binary ferroborate $Nd_{0.75}Dy_{0.25}Fe_3(BO_3)_4$ in the temperature range of 7–295 K with 532 nm (18797 cm^{-1}) laser excitation. The performed analysis of the polarized Raman spectra revealed the bands assigned to phonon, magnetic, and electronic excitations. The temperature evolution of these quasiparticle excitations has allowed us to ascertain the intricate coupling and interplay between lattice, magnetic, and electronic degrees of freedom. Analysis of the measured Raman spectra made it possible to identify all A_1 and E phonon modes predicted by the group-theoretical analysis. The splitting energies between the LO and TO components of the polar E phonons were determined. Below the magnetic ordering temperature of the Fe sublattice, T_N, we have revealed a multiple peaked two-magnon excitation. Analyzing the temperature evolution of low-frequency modes in the spectra, we also identified modes that are associated with electronic transitions between the crystal field levels of the Nd^{3+} ions with ground-state $^4I_{9/2}$ and of the Dy^{3+} ions with ground-state $^6H_{15/2}$ multiplets. In addition to the already known temperatures of magnetic transitions, analysis of the temperature behavior of low-frequency phonon and electronic excitations made it possible to establish a temperature $T^* = 100$ K, presumably associated with local distortions of the crystal lattice. The presence of this temperature is confirmed by our ultrasonic study. A group of intense bands observed in the frequency range 1700–2200 cm^{-1} has been associated with the mixed low-lying electronic Raman transitions $^4I_{9/2} \rightarrow {}^4I_{11/2}$ and the high-energy luminescence ones $^4G_{5/2}+{}^2G_{7/2} \rightarrow {}^4I_{9/2}$ for the Nd^{3+} ion.

1. INTRODUCTION

The rare-earth ferroborates $RFe_3(BO_3)_4$, with R = Y, La–Nd, and Sm–Er, gained considerable attention during the last few years due to the extraordinary physical properties of the members of this family caused by the coupling of the magnetic, electric, and lattice degrees of freedom, specifically, multiferroic effects in some of them as to their promising technological application.[1] The specific nature of the optical, magnetic, and magneto-electric properties of rare-earth ferroborates is due to the exchange interaction between the magnetic and electric subsystems of the iron and rare-earth ions.[1,2] The presence of two magnetic sublattices gives the opportunity for a variety of magnetic ordering phenomena, since the temperature-dependent competition between the anisotropy of these sublattices leads to different magnetic structures and may induce spin reorientations and metamagnetic behavior.[3]

The recent tendency to study ferroborates with two types of rare-earth ions is related to the fact that the substitution can significantly change the properties of magnetic/electronic subsystems, as well as their interaction. Today, one of the most interesting rare-earth binary ferroborates system is that of $Nd_{1-x}Dy_xFe_3(BO_3)_4$. The first results of studying these compounds, specifically $Nd_{0.75}Dy_{0.25}Fe_3(BO_3)_4$, appeared a few years ago.[4,5] Magnetic

susceptibility measurements revealed two magnetic phase transitions: the first at $T_N = 32$ K, which was attributed to a transition into the antiferromagnetic state with easy-plane anisotropy, and the second at $T_R = 25$ K, which corresponds to a spin-reorientation transition into the state with easy-axis.[4] The behavior of the magnetization and specific heat of this compound was studied in Ref. 5. The authors observed the presence of four features at $T_N = 32$ K, $T_1 = 24$ K, $T_2 = 22$ K, and $T_3 = 16$ K both in the temperature dependence of the magnetization and of the specific heat.

It is of interest to study the role of all interacting subsystems in the formation of unique physical properties of rare-earth binary ferroborates, which, in particular, can be tuned by changing the temperature. Here we present the Raman scattering study of the $Nd_{0.75}Dy_{0.25}Fe_3(BO_3)_4$ single crystal. Raman spectroscopy is a highly sensitive and informative nondestructive method allowing simultaneous probing of the elementary quantum excitations. Raman spectra of the $Nd_{0.75}Dy_{0.25}Fe_3(BO_3)_4$ single crystal were measured within the wide frequency range 12–2500 cm^{-1} at temperatures from 7 to 295 K. The performed analysis of polarized Raman spectra revealed the bands assigned to phonon, magnetic, and electronic excitations. The analysis of the polarized phonon spectra has revealed all A_1 and E phonon modes predicted by the group-theory analysis. The phonon bands have been classified into either internal or external modes. We have revealed the different temperature evolutions of the internal as well as external modes. An analysis of the temperature behavior of phonon excitations made it possible to reveal the presence of a strong interaction of the magnetic and lattice subsystems. An important feature of the iron spin ordering is the observation of a structured band ascribed to two-magnon excitation in the low-frequency part of the spectra at temperatures below T_N. Another important feature observed in low-frequency Raman spectra is excitations, the analysis of the frequency and temperature behavior which made it possible to classify them as electronic transitions between the levels within both the $^4I_{9/2}$ ground state of Nd^{3+} and the $^6H_{15/2}$ ground state of the Dy^{3+} ions.

A group of intense bands observed in the frequency range 1700–2200 cm^{-1} has been associated with the mixed Raman electronic transition $^4I_{9/2} \rightarrow {}^4I_{11/2}$ and the luminescence transitions $^4G_{5/2} + {}^2G_{7/2} \rightarrow {}^4I_{9/2}$ in the Nd^{3+} ion, which have the different temperature evolution. The bands' intensities of both electronic transitions increase, reaching a maximum at T_N with cooling. The contours of the electronic Raman bands were detected at low temperatures in contrast to the luminescence bands. The complicated temperature evolution of the electronic bands might be explained by the strong exchange coupling of the magnetic sublattices saturated by the different types of the magnetic ions below T_N. That significantly distorts the electronic structure of the Nd^{3+} ion.

In the present work, we studied the elastic properties of the title compound by the ultrasonic method also. Studying the behavior of the elastic characteristics of the crystals with a strong magnetoelastic interaction makes it possible to obtain information not only on the state of the phonon subsystem and structural phase transitions, but also to analyze the state of the magnetic subsystem. In particular, phase transitions of a purely magnetic nature (both spontaneous and induced by a magnetic field) often manifest themselves as pronounced anomalies in the behavior of the velocity and absorption of acoustic modes of magnetic crystals.[6]

2. EXPERIMENTAL DETAILS

Single crystals of $Nd_{0.75}Dy_{0.25}Fe_3(BO_3)_4$ have been grown from the solutions-melts based on bismuth thrimolibdates according to the technology described in Ref. 5. The orientation of the sample was performed by the x-ray back-reflection method (Laue method).

The Raman measurements were performed in a back- scattering geometry, using a triple spectrometer (Dilor-XY-500) equipped with liquid nitrogen cooled CCD (Horiba Jobin-Yvon, Spectrum One CCD-3000V). Raman spectra were excited with 532 nm radiation of solid-state Nd:YAG laser. The laser power was set to 3 mW with a spot diameter on the crystal of approximately 100 μm to avoid the heating effect. All measurements were carried out in an evacuated closed-cycle cryostat in the temperature range of 7–295 K.

The high-temperature crystal structure of $RFe_3(BO_3)_4$ compounds belongs to the trigonal space group $R32$.[7] Three kinds of coordination polyhedra present in this structure: trigonal RO_6 prisms, FeO_6 octahedra, and two types of planar triangular BO_3 groups — equilateral $B1O_3$ and isosceles $B2O_3$. The FeO_6 octahedra share edges forming nearly independent helicoidal chains that run parallel to the c axis (see Fig. 1). At cooling the crystal structure of the parent $NdFe_3(BO_3)_4$ compound remains trigonal $R32$ down to at least 2 K.[8] On the contrary, $DyFe_3(BO_3)_4$ reveals a first-order phase transition from the high-temperature $R32$ structure to the low-temperature $P3_121$ one at $T_S \approx 280$ K.[3,9] As for the $Nd_{0.75}Dy_{0.25}Fe_3(BO_3)_4$ binary compound, we did not find any literature data about the structural phase transition at the temperature of the present Raman studies.

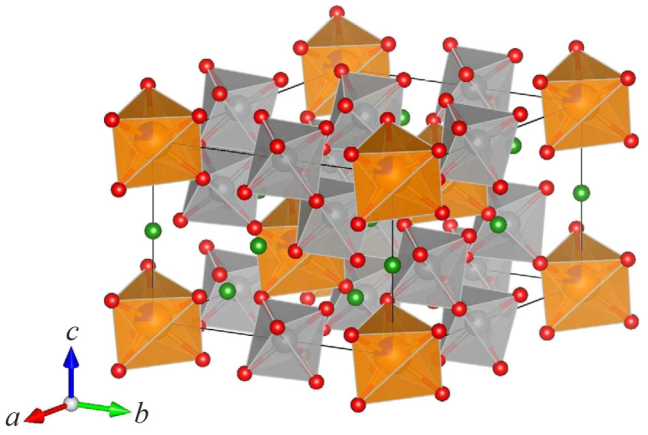

FIG. 1. The crystalline structure of the $Nd_{0.75}Dy_{0.25}Fe_3(BO_3)_4$ unit cell. The FeO_6 octahedra and $Nd_{0.75}/Dy_{0.25}O_6$ trigonal prisms are presented in grey and orange colors, respectively. O and B atoms are shown in red and green colors, respectively. The crystal structure is drawn using VESTA software.[10]

For the high-temperature structure, $R32$ of $RFe_3(BO_3)_4$ theory-group analysis gives $\Gamma_{vibr} = 7A_1$ (Raman) + $12A_2$ (IR) + $19E$ (Raman) optical vibrational modes, where the number of external and internal (related to the vibrations of BO_3 groups) vibrational modes is $\Gamma^{ext}_{vibr} = 3A_1 + 11E$ and $\Gamma^{ext}_{vibr} = 4A_1 + 8E$, respectively.[8] The doubly degenerated E modes are polar and both IR and Raman active.

Due to the shape of the samples, our Raman experiments were performed with light incident parallel and perpendicular to the C_3 axis. The Raman spectra were taken in $c(aa)\bar{c}$, $c(ab)\bar{c}$, $b(ac)\bar{b}$, and $b(cc)\bar{b}$ scattering configurations, where the c axis coincides with the C_3 axis, and the a and b axes are mutually orthogonal and located in the ab plane. As a result, with the exciting light propagating along the c axis ($\mathbf{k} \parallel c$) the TO modes were probed, while the $\mathbf{k} \perp c$ configuration gave the pure LO modes.

The experimental sample for acoustic research was cut from the single crystal consisting of a transparent hexahedral prism, green in color and of the order of 5 mm high, in a direction close to the C_3 axis and had the size of 1.5 mm (along the C_3 axis), 1 mm (along the C_2 axis), and 1 mm ($\perp$ to the C_2 axis). The working faces of the samples were polished with the corundum powder. Plane-parallelism of the faces was controlled by the optimeter and was not lower than 0.003°.

The crystal elastic characteristics were studied using a pulsed ultrasonic method for simultaneous measurement of the velocity and attenuation of sound waves propagating in the crystal. Measurements of the relative changes of the velocity and attenuation of the sound were performed using the automated apparatus described in Ref. 11. We investigated the behavior of the velocity of transverse acoustic modes depending on temperature. The precision of the measurements with the thickness of samples ~ 0.5 mm was about ~ 10^{-4} for the velocity and the working frequency was 54.3 MHz. The range of the temperature was 1.7–120 K.

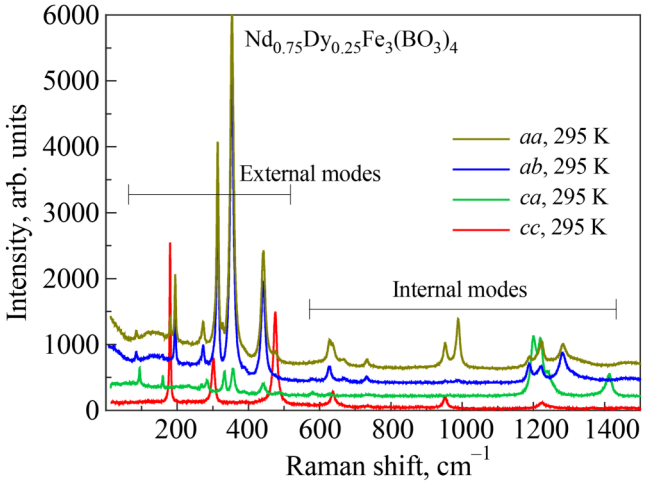

FIG. 2. The room-temperature Raman spectra of the $Nd_{0.75}Dy_{0.25}Fe_3(BO_3)_4$ taken in the different polarization configurations. The regions assigned to the external optical vibrations and the internal BO_3 vibrations are indicated by the horizontal bars.

3. EXPERIMENTAL RESULTS

3.1. Phonon scattering

The room-temperature Raman spectra of the $Nd_{0.75}Dy_{0.25}Fe_3(BO_3)_4$ for all studied polarization configurations are presented in the frequency region up to 1500 cm^{-1} in Fig. 2. There are phonon modes with the linewidth of not exceeding 15 cm^{-1}. The assignment of the phonon modes to the external and internal optical BO_3 vibrations was performed on the example of Raman analysis of rare-earth borates[8] and they are indicated by the horizontal bars in Fig. 2. The sharpness of the observed phonon modes indicates the high quality of the studied single crystal. The spectra show a strong deviation in the different scattering geometry. The frequencies of the observed Raman-active vibrational modes in $Nd_{0.75}Dy_{0.25}Fe_3(BO_3)_4$, taken at $T = 295$ K together with these ones for pure $NdFe_3(BO_3)_4$, and their symmetry assignment[8] are presented in Table I. The origin of the mode marked with "*" is unclear. It is observed only in the case of $\mathbf{k} \parallel c$ with the parallel polarization of the incoming and scattered light. Perhaps it is a local mode that can be observed in the binary crystal.

To get more insight into the phonon dynamics, we analyzed the temperature dependence of the phonon line parameters. The phonon lines have the symmetric shape and were fit with

TABLE I. The comparative analysis of the observed vibrational modes for the high-temperature $R32$ structure of $Nd_{0.75}Dy_{0.25}Fe_3(BO_3)_4$ together with these ones for pure $NdFe_3(BO_3)_4$.[8] Data in brackets are from Ref. 12.

$Nd_{0.75}Dy_{0.25}Fe_3(BO_3)_4$, T = 295 K			$NdFe_3(BO_3)_4$[1,12]		
External modes ($3A_1 + 11E$)					
A_1	E_{TO}	E_{LO}	A_1	E_{TO}	E_{LO}
179.9	85.1	94.6	180(176)	89	93 (90)
301.1	159	159.6	298 (297)		159 (155)
327*	194.2				193 (190)
475		230.5	473 (470)	(221)	232 (224)
	264.5	268.5		260 (257)	266 (265)
	272.7	283.6		272 (269)	281 (278)
	313.9	332.4		312 (308)	332 (328)
	353.3	356.8		354 (349)	356 (351)
	387.8	387.8			384
	441.4	441		(436)	439 (436)
		487.9		475	488 (485)
Internal modes ($4A_1 + 8E$)					
A_1	E_{TO}	E_{LO}	A_1	$E(E_{TO}/E_{LO})$	
637	580.9	581.2	636 (947)	579 (-/576)	
952	627.3	627	950	625 (622/622)	
984.6	667.7		990 (985)	669	
1223	732.1	736.5	1220 (1219)	734 (730/-)	
				968	
	988.5	1200.4		1195 (1182/1194)	
	1188.1	1219.4		1218 (-/1214)	
	1216	1240.7		1244 (-/1238)	
	1283.2			1260 (1280/-)	
		1411.9		1413 (-/1407)	

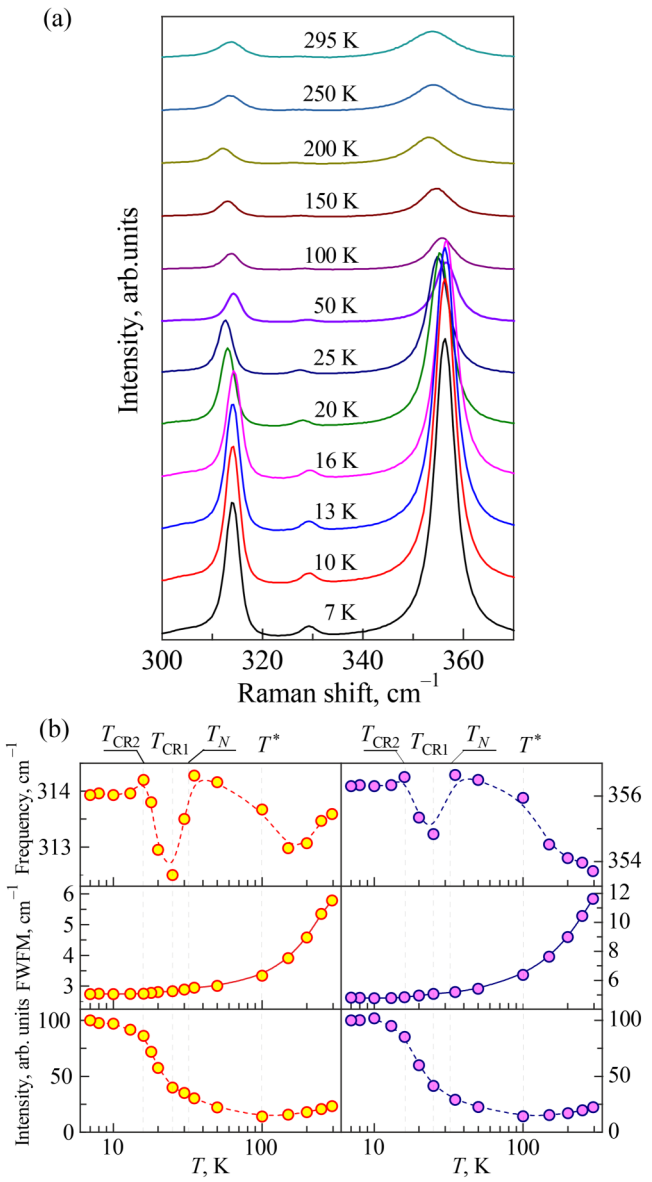

FIG. 3. (a) The temperature evolution of Raman spectra in the region of 300–370 cm^{-1}. (b) Temperature dependences of the peak position, linewidth, and normalized intensity of two external phonon modes (313.9 and 356.8 cm^{-1}) of $Nd_{0.75}Dy_{0.25}Fe_3(BO_3)_4$. The dashed lines indicate the B-spline fitting. The vertical dashed lines indicate the magnetic transitions, T_N, T_{CR1}, and T_{CR2}, and structural distortion, T, temperatures.

Lorentzian profiles in the whole investigated temperature range. Figure 3(a) shows the frequency region of 300–370 cm^{-1} containing the most pronouncing external modes: 313.9 and 356.8 cm^{-1}. The characteristic parameters on the Lorentzians [peak position, full width at half maximum (FWHM) and normalized intensity] are presented in Fig. 3(b). An analysis of the temperature behavior

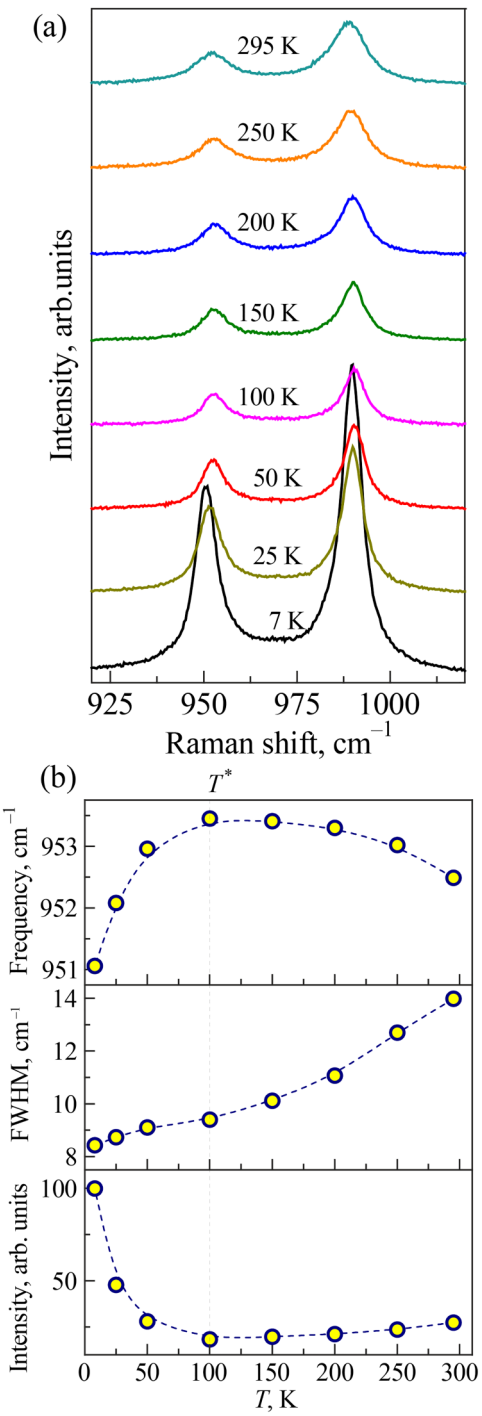

FIG. 4. (a) The temperature evolution of Raman spectra in the region of 920–1020 cm^{-1}. (b) Temperature dependences of frequency, linewidth, and normalized intensity of the internal BO_3 phonon mode at 952 cm^{-1}. The dashed lines indicate the B-spline fitting.

of these external phonon modes reveals three anomalies around the characteristic temperature points: $T_{CR2} = 16$ K, $T_{CR1} = 26$ K, $T_N = 32$ K, and $T^* = 100$ K [Fig. 3(b)]. The notable change in the phonon peak positions near the magnetic transition points is explained by the strong spin-phonon coupling. The linewidth demonstrates the typical exponential dependence that can be described in terms of an anharmonic model of phonon decay processes.[13] The peak intensity increases up to T_{CR2} with cooling and comes to the plateau. It is determined by the change of the dielectric function, i.e., the polarizability, and suggests the delicate nature of the electronic band reconstruction.

Figure 4(a) shows the measured temperature-dependent Raman spectra in the region of 920–1020 cm^{-1}. The performed polarization analysis suggests that the pronounced 952 cm^{-1} mode can be assigned to the internal mode BO_3 vibrations.[8] Figure 4(b) collects the temperature-dependent parameters of the 952 cm^{-1} mode: peak position, FWHM and normalized intensity. In contrast to the temperature evolution of the external modes presented in Fig. 3(b), the internal 952 cm^{-1} BO_3 phonon mode shows the deviation from the typical behavior only at one temperature, $T^* = 100$ K. The anomaly in the same temperature $T^* = 100$ K was revealed in the velocity and absorption behavior of the transverse acoustic modes of the related compound $Nd_{0.6}Dy_{0.4}Fe_3(BO_3)_4$.[14] The authors attributed this anomaly to the structural distortions induced by the Dy^{3+} ions.

We now turn to the acoustic characteristics of the $Nd_{0.75}Dy_{0.25}Fe_3(BO_3)_4$ crystal. The low-temperature behavior of the velocities of acoustic modes have been studied earlier and published in Refs. 15–17. All transverse velocities show anomalies at the temperatures $T_N = 32$ K — the kink, $T_{CR1} = 25$ K, and $T_{CR2} = 16$ K — jumps ~ 0.5% corresponding to phase transitions in the magnetic subsystem of the crystal, see Fig. 5. At the $T_N = 32$ K, the

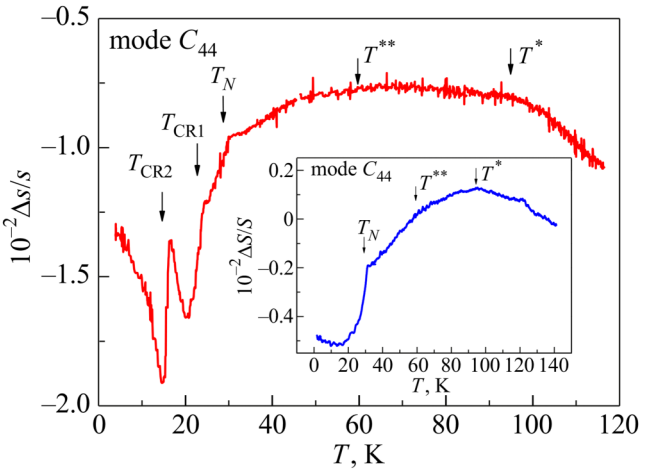

FIG. 5. The temperature behavior of relative changes of the velocity ($\Delta s/s$) of the transverse acoustic mode C_{44} (**q** || *c*, **u** || *b*) of the $Nd_{0.75}Dy_{0.25}Fe_3(BO_3)_4$. Inset: The temperature behavior of the velocity of the transverse acoustic mode C_{44} of the $Nd_{0.6}Dy_{0.4}Fe_3(BO_3)_4$.[13]

compound transforms into a magnetically ordered state, and a collinear antiferromagnetic structure with an "easy-plane" anisotropy is realized. The temperature $T_{CR2} = 16$ K corresponds to the transition to the easy-axis phase, which exists down to the lowest temperatures. In the range of 25–16 K, a certain intermediate "oblique" phase is realized, the magnetic structure of which has not yet been finally determined.

In the present work, we have analyzed the behavior of acoustic characteristics in the wider temperature range of 2–120 K, including the region of the paramagnetic state (Fig. 5). At temperatures from 120 to 100 K, the velocities of some of transverse modes [C_{44} mode (**q** || c, **u** || b), mode (**q** || *a*, **u** || c), and mode (**q** || *a*, **u** || b), where **q** is the wave vector, and **u** is the polarization] with decreasing temperature, i.e., they exhibit typical solid-state behavior without any anomalies. With further cooling, in the range between $T^* \approx 100$ K and $T^{**} \approx 60$ K, a plateau is observed in the behavior of the velocities, which below $T^{**} \approx 60$ K is replaced by a noticeable softening. As an example, Fig. 5 shows the temperature dependence of the relative changes in the velocity of the transverse acoustic C_{44} mode.

Since no peculiarities in the behavior of the heat capacity and magnetization in the paramagnetic temperature range were recorded,[5] we assumed that the anomalous behavior of the acoustic modes' velocities is associated with changes in the phonon (but not magnetic) subsystem of the crystal. The fact that not all, but only some of the possible acoustic modes demonstrate anomalous behavior above the Neel temperature, in the absence of well-localized features at a specific temperature, gives grounds to assert that a structural phase transition with a change in the space symmetry group does not occur in the crystal. We can only talk about possible lattice distortions associated with sufficiently high dysprosium ions content in the compound. To remind, at the temperature ≈280 K the first order phase transition ($R32 \rightarrow P3_121$) is realized in dysprosium ferroborate.[3,9] Note that we observed a similar behavior of the temperature dependences of velocities of some transverse modes in the related compound $Nd_{0.6}Dy_{0.4}Fe_3(BO_3)_4$.[14] However, in this case, with temperature decreasing, the velocity of the C_{44} mode increased, reaching a maximum at $T^* \approx 100$ K, and then softened, experiencing a kink at $T^{**} \approx 60$ K, up to a jump at T_N (see inset in Fig. 5).

3.2. Magnetic excitations

In contrast to pure neodymium and dysprosium ferroborates, $Nd_{0.75}Dy_{0.25}Fe_3(BO_3)_4$ has a complex phase diagram with a cascade of magnetic phase transitions at temperatures,[15–17] which is a manifestation of the interplay of magnetic sublattices formed by the Nd^{3+}, Dy^{3+}, and Fe^{3+} ions. Raman spectroscopy is a sensitive technique for probing the excitations related to long- and short-range magnetic interactions as well as magnetic fluctuations. The previously held spectroscopic study of the rare-earth ferroborates $RFe_3(BO_3)_4$ (Gd, Tb, Nd, Er, and Y) showed that the Fe-sublattice ordering leads to a strong suppression of the broad low-energy magnetic scattering and to the appearance of a two-magnon signal in the spectra.[8] A similar picture of magnetic excitations was observed in the Raman study of $SmFe_3(BO_3)_4$.[18]

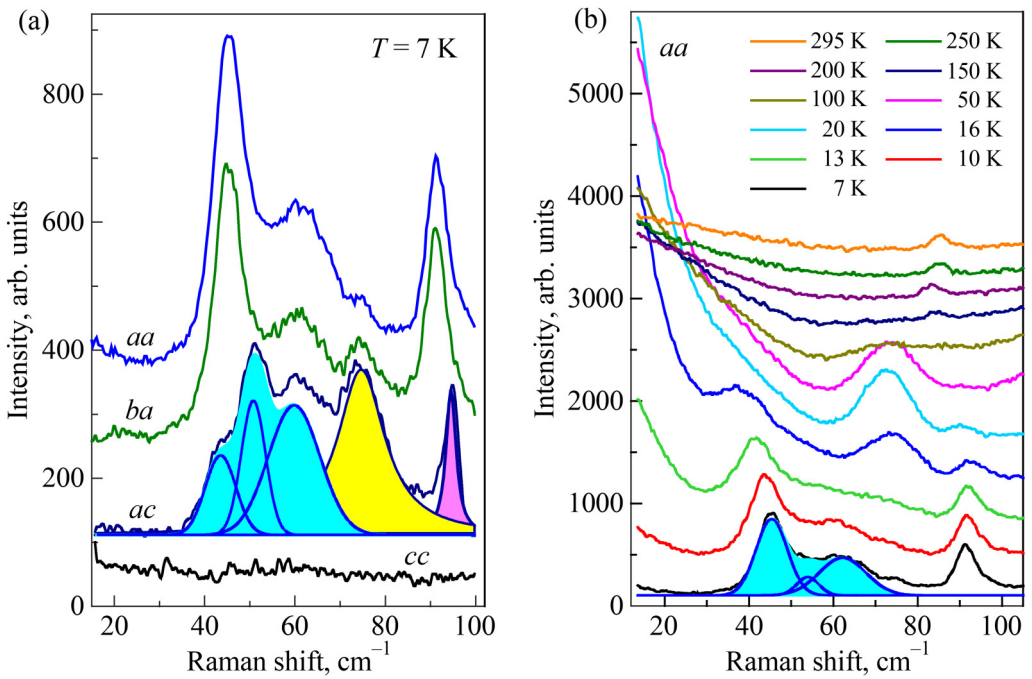

FIG. 6. (a) Low-frequency part of the Raman spectra of $Nd_{0.75}Dy_{0.25}Fe_3(BO_3)_4$ taken at $T = 7$ K in four polarization configurations. (b) Temperature-dependent low-frequency Raman spectra taken in *aa* polarization. Cyan shading in (a) and (b) depicts the multiple peaked two-magnon signal at $T = 7$ K.

Magnetic scattering in $Nd_{0.75}Dy_{0.25}Fe_3(BO_3)_4$ is evident as quasielastic scattering (QS, $E \approx 0$) and as two-magnon scattering, both with characteristic polarization and temperature dependences in intensity and frequency.

Figure 6(a) zooms into the low-frequency part of the Raman spectra of $Nd_{0.75}Dy_{0.25}Fe_3(BO_3)_4$ measured at $T = 7$ K in different polarization configurations. A multiple peaked broad band with peaks at 43.5, 50.8, and 59.8 cm^{-1} is present in the spectra with *aa, ba,* and *ac* polarization configurations. No evidence of magnetic scattering is found when polarizations of the incident and scattered lights are parallel to the *c* axis. This observed structured band can be attributed to two-magnon Raman scattering, arising from a double spin-flip process involving neighboring sites. In compounds with complex lattice structure, several magnetic ions per unit cell and competing magnetic exchange interactions the two-magnon Raman spectrum is expected to comprise a few bands.[19] In the case of $RFe_3(BO_3)_4$, one should expect the presence of three bands in the two-magnon spectrum arising from three magnon branches representing spin excitations on the iron chains. Indeed, qualitatively similar two-magnon spectra were observed in the magnetically ordered phase of several $RFe_3(BO_3)_4$ compounds, evidencing that the compositional and structural differences between them do not strongly affect the magnetism and the magnetic excitation spectra.[8]

Figure 6(b) shows the temperature evolution of the low-frequency part of the Raman spectra of $Nd_{0.75}Dy_{0.25}Fe_3(BO_3)_4$ measured in the *aa* polarization configuration. The two-magnon spectrum behaves as expected for the conventional magnetic system: its intensity is suppressed; the frequency position softens continuously and excitation hides under wing of the QS line on the approach to the Neel temperature with heating. The temperature behavior of QS signal will be discussed below.

A striking feature of the magnetic scattering in $Nd_{0.75}Dy_{0.25}Fe_3(BO_3)_4$, as shown in Fig. 7, is the absence of a QS

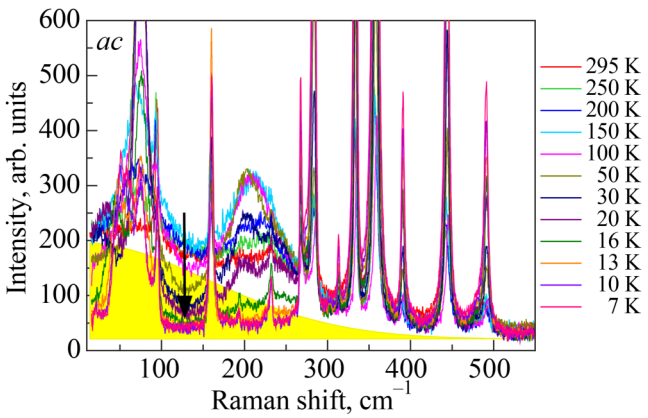

FIG. 7. Temperature evolution of the magnetic background continuum in $Nd_{0.75}Dy_{0.25}Fe_3(BO_3)_4$ taken in the *ac* polarization configuration. Yellow shading depicts the continuum at $T = 295$ K. The black arrow marks the decrease in the magnetic background continuum upon cooling.

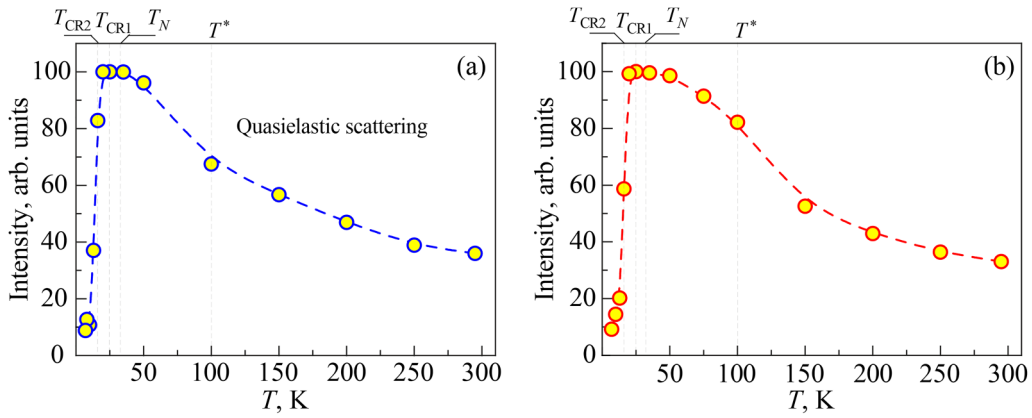

FIG. 8. (a) Temperature-dependent normalized intensity of the quasielastic scattering extracted from the Raman spectra of $Nd_{0.75}Dy_{0.25}Fe_3(BO_3)_4$. (b) Temperature evolution of the normalized intensity of the sum of the 111.9 and 149 cm^{-1} electronic modes. We present here the sum of the intensities of the two modes, since at temperatures above T^* they overlap, forming one broad band. The dashed lines indicate the B-spline fitting.

signal in the *ac* scattering geometry and persistence of the wide magnetic scattering in an anomalous shape in a wide temperature range. Systematic analysis of this continuum may provide crucial informations about the underlying long-wavelength dynamical spin fluctuations. The Raman response shows a significant build-up of the intensity below ~ 500 cm^{-1} on increasing the temperature from $T = 20$ K up to $T = 150$ K, and it remains unchanged upon further heating. This characteristic scattering feature is different from the conventional magnetic system, where quantum spin fluctuations quenched to zero quickly below T_{nN} in the ordered phase also,[20] but decay exponentially fast above T_N. Similar wide magnetic scattering signal extending up to ~ 500 cm^{-1} (not shown here) was observed also in the *aa* and *ab* scattering configurations and was fully absent in the *cc*. At present, one cannot draw a definite conclusion, but the results do strongly suggest that short-range order correlations in the spin system survive up to quite high temperatures. Most likely interplay between the low dimensionality, magnetic frustration, and strong interaction between spin, electron and lattice subsystems are responsible for the observed unique behavior of the magnetic scattering up to several times T_N and deserves further studies. Note that a magnetic continuum of a similar shape was observed in Raman studies of a strongly spin-orbit-coupled Mott insulator Sm_2ZnIrO_6[21] and was interpreted as a characteristic feature of the Kitaev physics.

We will turn now to the QS observed in the *aa* [Fig. 6(b)] and *ab* Raman spectra of $Nd_{0.75}Dy_{0.25}Fe_3(BO_3)_4$. Temperature evolution

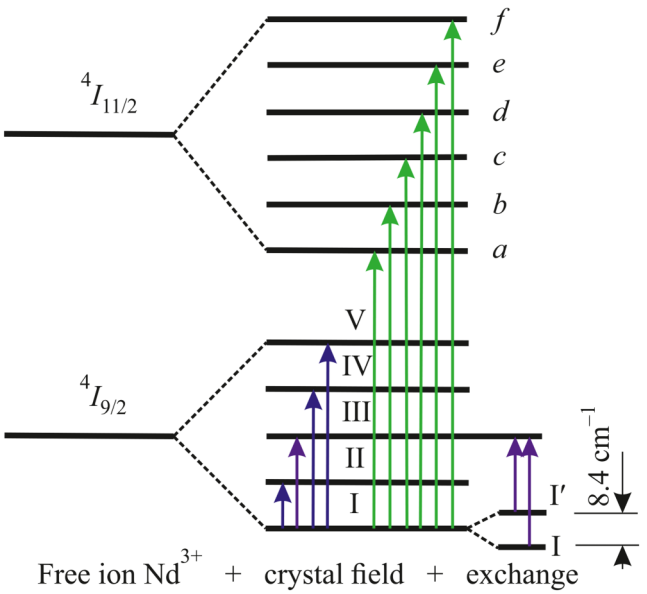

FIG. 9. Scheme of the Nd^{3+} ions levels split by the CF and of optical transitions.

TABLE II. Measured at $T = 50$ K[22] and calculated[22,23] crystal-field energies Δ (cm^{-1}) = E_i - E_I of the $^4I_{9/2}$ Nd^{3+} and the $^6H_{15/2}$ Dy^{3+} multiplets in $NdFe_3(BO_3)_4$ and $Nd_{0.75}Dy_{0.25}Fe_3(BO_3)_4$.

$^{2S+1}L_j$,R	Compound, Ref.	$\Delta = E_i$ - E_I, cm^{-1}
$^4I_{9/2}$, Nd^{3+}	$NdFe_3(BO_3)_4$,[22] Theory	I — 0, II — 66,
	$NdFe_3(BO_3)_4$,[22] Experiment	III — 141, IV — 220,
	$Nd_{0.75}Dy_{0.25}Fe_3(BO_3)_4$,[23] Theory	V — 310 I — 0, II — 65, III — 141, IV — 221, V — 322
		I — 0, II — 79.2, III — 165.8, IV — 261
$^6H_{15/2}$, Dy^{3+}	$Nd_{0.75}Dv_{0.25}Fe(BO_3)_4$,[23] Theory	I* — 0, II* — 21.9, III *— 108.6, IV* — 207

TABLE 3. Frequencies of the observed electronic transitions extracted from Raman spectra of $Nd_{0.75}Dy_{0.25}Fe_3(BO_3)_4$ together with these ones for pure $NdFe_3(BO_3)_4$ (Ref. 22).

Line [Fig. 11(c)]	$Nd_{0.75}Dy_{0.25}Fe_3(BO_3)_4$, $T = 50$ K, present study	$NdFe_3(BO_3)_4$, $T = 50$ K [22]
	Frequency of $^4I_{9/2} - {}^4I_{11/2}$ [cm^{-1}]	
1′	1908	1949
2′	1944	1955
3′	1981	1979
4′	2011	2053
5′	2053	2087
6′	2095	2131

of its integrated intensity is shown in Fig. 8(a). With temperature decreasing down to T_N, the intensity of quasielastic scattering increases indicating the rise of the short-range correlations in the subsystems. In the temperature range between T_N and T_{CR1} the intensity of the QS is nearly constant and than it decreases dramatically. A similar QS signal, identified as a "paramagnon" scattering, was observed and discussed in Ref. 8 in the study of several members of the $RFe_3(BO_3)_4$ family. The origin of this unprecedentedly interesting paramagnon scattering continuum was not attributed to the usual energy diffusion observed in a variety of other magnetic system, but, presumably, indicates the presence of short-range spin-spin correlations arising from the low-dimensional nature of these compounds and the strong spin-lattice interactions. We do not exclude also the contribution of electronic correlations to the formation of the QS signal. This may follow from the temperature behavior of the intensity of the crystal field excitations between the levels of the ground-state $^4I_{9/2}$ multiplet of Nd^{3+}[22] and the ground-state $^6H_{15/2}$ multiplet of Dy^{3+},[23] similar to the QS signal [see Fig. 8(b), where intensity vs temperature for the sum of the 111.9 and 149 cm^{-1} electronic modes is shown]. Moreover, two low-energy electronic excitations overlap with the magnetic signal. It is well known that low-frequency excitations of different origin but with the same types of symmetry can interact resonantly and hybridize. Such interaction can lead to various effects, including energy shifts, asymmetric line Fano shapes, changing of spectral strengths, and violation of the selection rules, which complicate the correct interpretation of experimental data.

3.3. Electronic excitations

Having discussed phonon and magnetic excitations, we turn to discussion of the local electronic crystal field probed through excitations on the Nd^{3+} and Dy^{3+} sites. The CF levels derived from the free-ion ground-state multiplet are often the most important ones to characterize a compound, since they may be used as a local probe and govern the magnetic, low-temperature thermal, and transport properties. The energies of Nd^{3+} CF levels in the parent $NdFe_3(BO_3)_4$ were calculated and experimentally found by analyzing the high-resolution temperature-dependent polarized absorption spectra in Ref. 22. The energies of the lower levels of the main multiplet of the Nd^{3+} and Dy^{3+} ions in $Nd_{0.75}Dy_{0.25}Fe_3(BO_3)_4$, split by the crystal field, were calculated in Ref. 23. Scheme of Nd^{3+} ions levels split by CF and of optical transitions are shown in Fig. 9. Table II lists measured and calculated CF energies of the Nd^{3+} ion

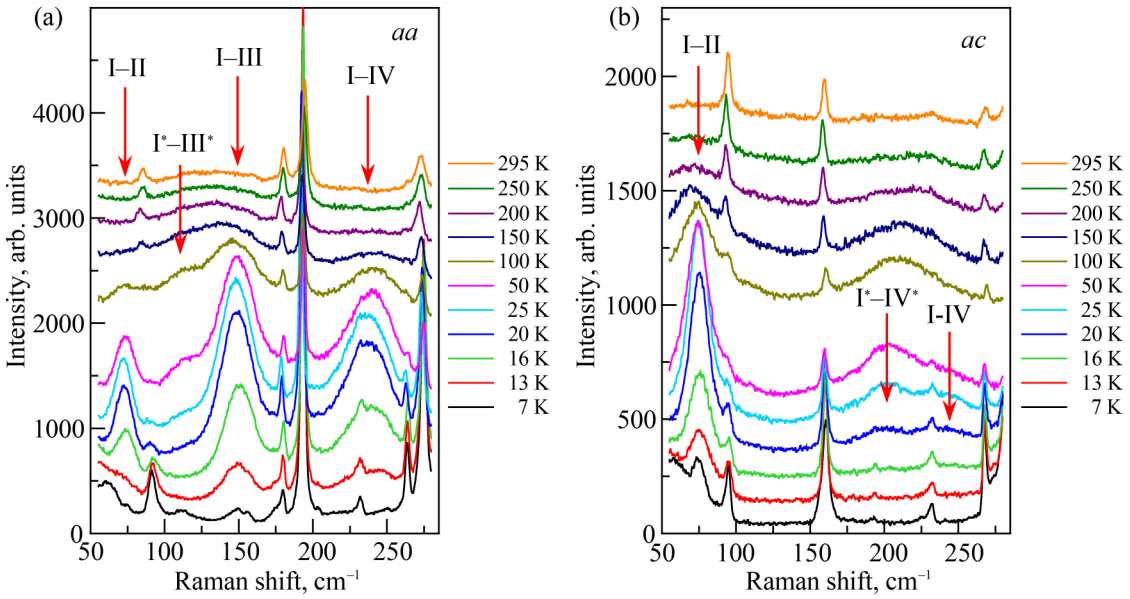

FIG. 10. (a) Temperature-dependent Raman spectra of $Nd_{0.75}Dy_{0.25}Fe_3(BO_3)_4$ measured in the frequency region of the low-frequency crystal field excitation in the *aa* (a) and *ac* (b) scattering configurations.

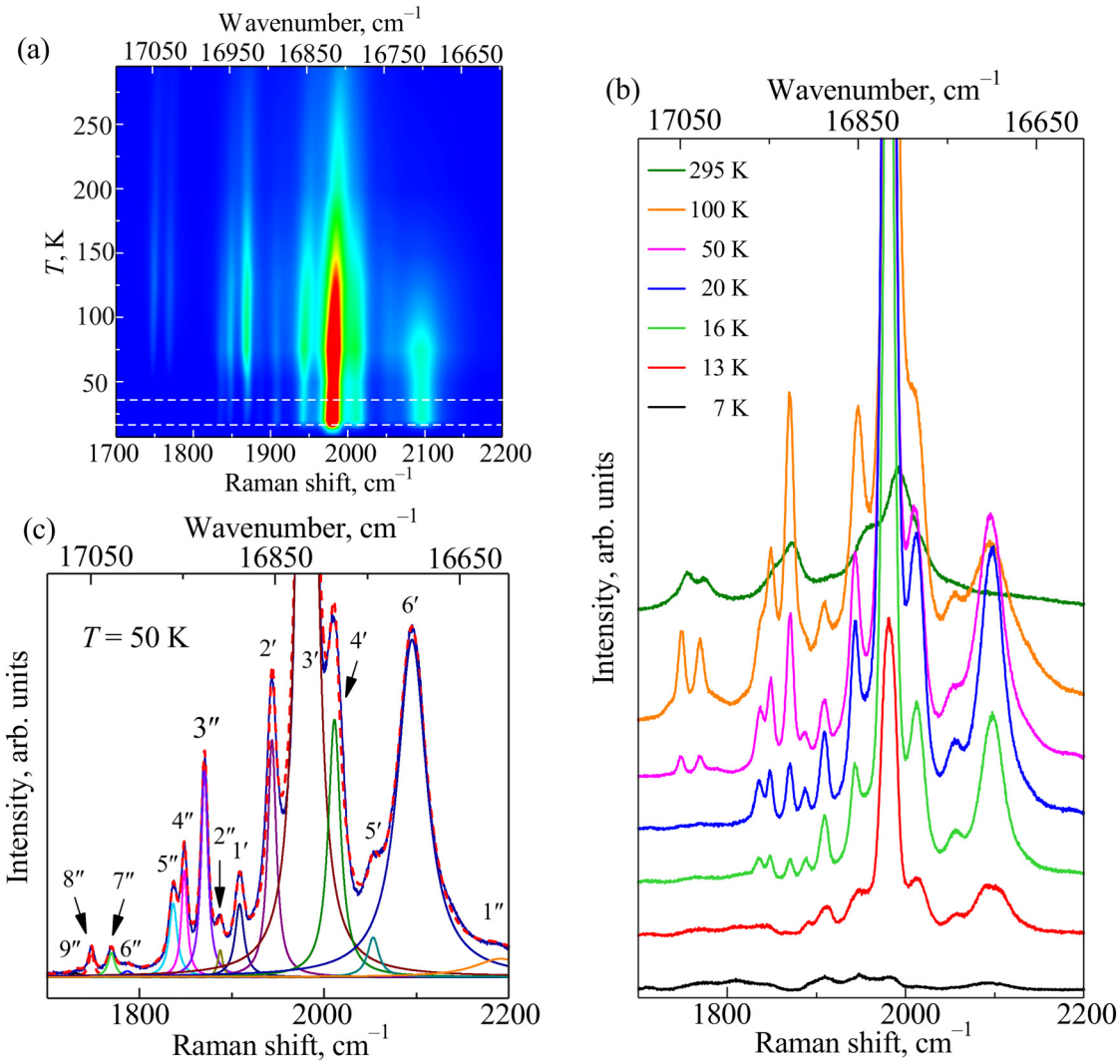

FIG. 11. (a) Color contour plot of the electronic bands' intensity in the temperature vs Raman shift plane. (b) Temperature evolution of Raman spectra ranging from 1700 to 2200 cm^{-1}. The spectra are shifted vertically for clarity. (c) Raman spectrum taken at $T = 50$ K is fitted to a sum of Lorentzian profiles. The blue solid thick line stands for the experimental data, the red dashed line represents the total sum of a fitting, and the thin solid colored lines are the individual fitting profiles. The lines labeled 1′ to 6′ may be assigned to the Raman $^4I_{9/2} \rightarrow {}^4I_{11/2}$ transitions and the lines marked 1" to 9" may be assigned to the luminescence transitions $^4G_{5/2} + {}^2G_{7/2} \rightarrow {}^4I_{9/2}$.

in $NdFe_3(BO_3)_4$[22] and calculated of the Nd^{3+} and Dy^{3+} ions in $Nd_{0.75}Dy_{0.25}Fe_3(BO_3)_4$.[23]

Figure 10 shows Raman spectra of $Nd_{0.75}Dy_{0.25}Fe_3(BO_3)_4$ measured at different temperatures in the frequency range of the Nd^{3+} transitions between the CF split levels of the $^4I_{9/2}$ ground state. It is clear seen that at temperatures $T > T^*$, the very wide bands (up to 70 cm^{-1}) centred at frequencies 67, 132, and 214 cm^{-1} are presented in the spectra. It is a reason to suppose that these lines are related to low-energy electronic transitions between the levels of the ground-state multiplets of rare-earth ions. Upon cooling through T^*, abrupt changes occur in the spectra: the bands narrow, the intensity sharply increase, and some of them are split. Comparing the experimentally observed energies of the CF excitations with those given in Table II of previous studies, we can attribute excitations with energies 73.4, 149, and 237.7 cm^{-1} to the transitions I-II, I-III, and I-IV between the CF levels of the Nd^{3+} ground-state $^4I_{9/2}$ multiplet and excitations with energies 73.4 and 201.5 cm^{-1} to the transitions I*-III* and I*-IV* between the CF levels of the Dy^{3+} ground-state $^6H_{15/2}$ multiplet, respectively. The temperature behavior of the low-frequency CF excitations is in a good agreement with behavior of optical and acoustic phonons, namely, once again indicates the presence of a specific temperature

T^*, at which, as we believe, changes in the parameters of the crystal field occur.

We turn attention to the next features observed in the low-frequency Raman spectra of $Nd_{0.75}Dy_{0.25}Fe_3(BO_3)_4$ (see Fig. 10):

(i) The Kramer's doublets of the Nd^{3+} ion split below the Neel temperature due to the magnetic exchange interaction and we observe the I-III CF mode splitting of the order of 8.4 cm^{-1} (see Figs. 9 and 10) which is in a good agreement with the data of Fig. 10(a).
(ii) Phonon lines having Fano profiles are superposed on a wide CF excitations, which indicate a strong electron-phonon interaction.
(iii) A splitting of some phonon modes and the appearance of new modes below T_N are observed. The discussion of the nature of this phenomenon is out of scope of the present study and is the object of our future studies. We suppose that one of the reasons of this phenomenon may be a zone folding in the magnetically ordered state.

Another intrigue observation arises in analyzing the high-frequency part of Raman spectra in the frequency range of 1700–2200 cm^{-1} [Fig. 11(a)]. It seems that these excitations can be attributed to electronic transitions between crystal field states of the Nd^{3+} ion.[22] A group of intense bands observed in the frequency range of 1700–2200 cm^{-1} can be associated with the mixed low-lying electronic Raman transition $^4I_{9/2}\rightarrow{}^4I_{11/2}$ and the high-energy luminescence transitions $^4G_{5/2}+{}^2G_{7/2}\rightarrow{}^4I_{9/2}$ of the Nd^{3+} ion [Fig. 11(b)]. These states cannot be simply separated and identified due to close energy proximity. Nevertheless, based on an analysis of the temperature behavior of the intensities of high-frequency excitations, we can assign the lines labeled from 1′ to 6′ [which corresponds to the transitions from $I\rightarrow a$ to $I\rightarrow f$ shown in Fig. 9] to the first group and the lines marked 1" to 9" to the second one [Fig. 11(c)]. The frequencies of the $^4I_{9/2}\rightarrow{}^4I_{11/2}$ electronic transitions measured at $T=50$ K for $Nd_{0.75}Dy_{0.25}Fe_3(BO_3)_4$ and pure $NdFe_3(BO_3)_4$[22] are presented in Table III. The small difference between the energies of the electronic transitions observed for both samples may be explained by the moderate disturbance induced by the Dy^{3+} ions. The energies of the transitions between $^4G_{5/2}+{}^2G_{7/2}$ levels and the levels within the main $^4I_{9/2}$ multiplet, $^4G_{5/2}+{}^2G_{7/2}\rightarrow{}^4I_{9/2}$ are 1″ — 16606, 2″ — 16910, 3″ — 16927, 4″ — 16948, 5″ — 16960, 6″ — 17010, 7″ — 17027, 8″ — 17052, and 9″ — 17066 cm^{-1}.

The temperature evolution of the electronic bands demonstrates a complicated character. The first group of the bands assigned to electronic transition $^4I_{9/2}\rightarrow{}^4I_{11/2}$, begins to show up below 200–175 K upon cooling. The bands' intensity increases, and the bands are subject to structuring as the temperature approaches T_N demonstrating a strong magnetoelectric effect. At around T_{CR2}, the intensity catastrophically falls down. The contours of the bands are detected at low temperatures. The temperature behavior of the above mentioned bands correlates to the temperature evolution of the low-frequency electronic bands caused by the electronic transitions between the levels of the $^4I_{9/2}$ multiplet of Nd^{3+} [Fig. 10(a)]. The second bands' group, caused by the electronic transitions from the mixed $^4G_{5/2}$ and $^2G_{7/2}$ multiplets to $^4I_{9/2}$ one, demonstrates a different behavior compared to the first one. This group is observed at room temperature. The bands intensity increases upon cooling down to about 100 K with subsequent falling. Below T_N, the bands belonging to the second group are not detectable. The complicated temperature evolution of the electronic bands might be explained by the appearance of the strong exchange coupling of the magnetic sublattices saturated by the different types of the magnetic ions below T_N. It can cause the structural change of the positions of the magnetic ions and the exchange splitting of Kramers doublets of the Nd^{3+} ion that significantly depletes the base levels. This, in turn, is reflected in the complicated temperature evolution of the electronic band intensities that was observed early in spectroscopic studies of the rare-earth crystal systems.[24,25] Unfortunately, we cannot restore the electronic structure of the $Nd_{0.75}Dy_{0.25}Fe_3(BO_3)_4$ single crystal using only Raman spectroscopy. Therefore, a more detailed study of the electronic structure of the $Nd_{1-x}Dy_xFe_3(BO_3)_4$ family using alternative optical methods is planned.

4. CONCLUSION

In summary, we have presented a Raman scattering study of the $Nd_{0.75}Dy_{0.25}Fe_3(BO_3)_4$ single crystal in a wide frequency region of 12–2500 cm^{-1} at temperatures 7–295 K. Raman studies were supported by the ultrasonic measurements. Raman spectroscopy is a highly sensitive and informative nondestructive method allowing probing simultaneously the elementary quantum excitations. The performed detailed analysis of polarized Raman spectra revealed the bands assigned to phonon, magnetic, and electronic excitations. All A_1 and E phonon modes, predicted by the group-theory analysis, were revealed in Raman spectra and have been classified into either internal or external modes. Phonon Raman scattering indicates strong spin-lattice coupling by revealing distinct anomalies at temperatures T^*, T_{CR1}, T_{CR2}, and T_N. Magnetic scattering in $Nd_{0.75}Dy_{0.25}Fe_3(BO_3)_4$ is evident as quasielastic scattering, wide magnetic background continuum, and multiple peaked two-magnon signal. The most surprising thing is that quasielastic scattering with a significant temperature dependence was observed in $\mathbf{k}||c$ geometry, i.e., with exciting light directed along the c axis of the crystal. Moreover, the temperature dependence of the QC signal intensity is practically identical to that of the magnetic susceptibility, χ_c, of easy-axis rare-earth ferroborates.[26] In the paramagnetic region, the magnetic susceptibility along the c axis obeys the Curie–Weiss law, and at $T<T_N$ it sharply decreases. At the same time, χ measured along the axes in the basal ab plane changes insignificantly with temperature. The observed in the Raman spectra bands at 73.4, 149, and 237.7 cm^{-1} have been assigned to electronic transitions between the CF levels of the Nd^{3+} ground-state $^4I_{9/2}$ multiplet and bands at 111.9 and 201.5 cm^{-1} — to the transitions between the CF levels of the Dy^{3+} ion with ground-state $^6H_{15/2}$ multiplet. A group of intense bands observed in the frequency range of 1700–2200 cm^{-1} has been associated with the mixed electronic Raman $^4I_{11/2}\rightarrow{}^4I_{9/2}$ and luminescence $^4G_{5/2}+{}^2G_{7/2}\rightarrow{}^4I_{9/2}$ transitions in the Nd^{3+} ion, which demonstrate different temperature behavior. The complicated temperature evolution of the high-frequency electronic bands is explained by the strong exchange competition coupling of the magnetic sublattices formed by the different types of the magnetic ions below T_N. The

study of the $Nd_{0.75}Dy_{0.25}Fe_3(BO_3)_4$ single crystal provides a new opportunity to examine the coupling effects of phonon, magnetic, and electronic subsystems.

ACKNOWLEDGMENTS

A. Yu. Glamazda thanks Dr. A. V. Peschanskii for fruitful discussions. P. Lemmens acknowledges funding by the DFG Excellence Cluster Quantum Frontiers, EXC 2123-390837967, DFG Le967/16-1, and DFG-RTG 1952/1.

REFERENCES

[1]A. N. Vasiliev and E. A. Popova, Fiz. Nizk. Temp. **32**, 968 (2006) [Low Temp. Phys. **32**, 735 (2006)].
[2]A. K. Zvezdin, S. S. Krotov, A. M. Kadomtseva, G. P. Vorob'ev, Yu. F. Popov, A. P. Pyatakov, L. N. Bezmaternykh, and E. A. Popova, JETP Lett. **81**, 272 (2005).
[3]C. Ritter, A. Pankrats, I. Gudim, and A. Vorotynov, J. Phys. Conf. Ser. **340**, 012065 (2012).
[4]Y. F. Popov, A. M. Kadomtseva, G. P. Vorob'ev, A. A. Mukhin, V. Y. Ivanov, A. M. Kuz'menko, A. S. Prokhorov, L. N. Bezmaternykh, and V. L. Temerov, Pis'ma Zh. Eksp. Teor. Fiz. **89**, 345 (2009).
[5]I. A. Gudim, E. V. Eremin, and V. L. Temerov, J. Crystal Growth **312**, 2427 (2010).
[6]G. A. Zvyagina, K. R. Zhekov, I. V. Bilych, A. A. Zvyagin, I. A. Gudim, and V. L. Temerov, Fiz. Nizk. Temp. **37**, 1269 (2011) [Low Temp. Phys. **37**, 1010 (2011)].
[7]J. A. Campa, C. Cascales, E. Gutierrez-Puebla, M. A. Monge, I. Rasines, and C. Ruiz-Valero, Chem. Mater. **9**, 237 (1997).
[8]D. Fausti, A. A. Nugroho, P. H. M. van Loosdrecht, S. A. Klimin, M. N. Popova, and L. N. Bezmaternykh, Phys. Rev. B **74**, 024403 (2006).
[9]E. A. Popova, N. Tristan, A. N. Vasiliev, V. L. Temerov, L. N. Bezmaternykh, N. Leps, B. Büchner, and R. Klingeler, Eur. Phys. J. B **62**, 123 (2008).
[10]K. Momma and F. Izumi, J. Appl. Crystallogr. **44**, 1272 (2011).
[11]E. A. Masalitin, V. D. Fil', K. R. Zhekov, A. N. Zholobenko, and T. V. Ignatova, Fiz. Nizk. Temp. **29**, 93 (2003) [Low Temp. Phys. **29**, 72 (2003)].
[12]Q. A. de Andrés, F. Agulló-Rueda, S. Taboada, C. Cascales, J. Campá, C. Ruiz-Valero, and I. Rasines, J. Alloys and Compounds **250**, 394 (1997).
[13]M. Balkanski, R. F. Wallis, and E. Haro, Phys. Rev. B **28**, 1928 (1983).
[14]G. A. Zvyagina, K. R. Zhekov, I. V. Bilych, A. A. Zvyagin, A. N. Bludov, V. A. Pashchenko, and I. A. Gudim, Fiz. Nizk. Temp. **40**, 187 (2014) [Low Temp. Phys. **40**, 146 (2014)].
[15]G. A. Zvyagina, K. R. Zhekov, I. V. Bilych, and A. A. Zvyagin, I. A. Gudim and L. N. Bezmaternyh, Fiz. Nizk. Temp. **36**, 352 (2010) [Low Temp. Phys. **36**, 279 (2010)].
[16]G. A. Zvyagina, K. R. Zhekov, A. A. Zvyagin, I. A. Gudim, and I. V. Bilych, Fiz. Nizk. Temp. **38**, 571 (2012) [Low Temp. Phys. **38**, 446 (2012)].
[17]G. A. Zvyagina, K. R. Zhekov, I. V. Bilych, A. A. Zvyagin, I. A. Gudim, V. L. Temerov, and E. V. Eremin, Fiz. Nizk. Temp. **39**, 1202 (2013) [Low Temp. Phys. **39**, 936 (2013)].
[18]A. V. Peschanskii and V. I. Fomin, and I. A. Gudim, Fiz. Nizk. Temp. **42**, 607 (2016) [Low Temp. Phys. **42**, 475 (2016)].
[19]M. G. Cottam and D. J. Lockwood, *Light Scattering in Magnetic Solids* (Wiley, New York, 1985).
[20]W. Hayes and R. Loudon, *Scattering of Light by Crystals* (Dover, New York, 2004).
[21]B. Singh, M. Vogl, S. Wurmehl, S. Aswartham, B. Büchner, and P. Kumar, Phys. Rev. Research **2**, 013040 (2020).
[22]M. N. Popova, E. P. Chukalina, T. N. Stanislavchuk, B. Z. Malkin, A. R. Zakirov, E. Antic-Fidancev, E. A. Popova, L. N. Bezmaternykh, and V. L. Temerov, Phys. Rev. B **75**, 224435 (2007).
[23]A. A. Demidov, I. A. Gudim, and V. V. Eremiv, JETP **114**, 259 (2012).
[24]B. Singh, M. Vogl, S. Wurmehl, S. Aswartham, B. Büchner, and P. Kumar, Phys. Rev. Research **2**, 023162 (2020).
[25]E. P. Chukalina, D. Y. Kuritsin, M. N. Popova, L. N. Bezmaternykh, S. A. Kharlamova, and V. L. Temerov, Phys. Lett. A **322**, 239 (2004).
[26]A. M. Kadomtseva, Y. F. Popov, G. P. Vorob'ev, A. P. Pyatakov, S. S. Krotov, K. I. Kamilov, V. Y. Ivanov, A. A. Mukhin A. K. Zvezdin, A. M. Kuz'menko, L. N. Bezmaternykh, I. A. Gudim, and V. L. Temerov, Fiz. Nizk. Temp. **36**, 640 (2010) [Low Temp. Phys. **36**, 511 (2010)].